Extended Abstracts of the 2003 International Conference on Solid State Devices and Materials, Tokyo, 2003, pp. 322-323

E-5-3

Investigation of Electron Transition Energy for Vertically Coupled InAs/GaAs Semiconductor Quantum Dots and Rings

Yiming Li[1,2] and Hsiao-Mei Lu[3]

[1]Department of Nano Device Technology, National Nano Device Laboratories, Hsinchu 300, Taiwan
[2]Microelectronics and Information Systems Research Center, National Chiao Tung University, Hsinchu 300, Taiwan
[3]Department of Bioengineering, University of Illinois at Chicago, Chicago, Illinois 60612, USA
Phone: +886-930-330766 E-mail: ymli@mail.nctu.edu.tw

1. Introduction

Semiconductor nanostructures possess fascinating physical properties and are attractive to diverse applications, such as quantum computing, lasers, infrared photo detectors, and spintronics. Single quantum dot (or ring) has been a subject of intensely studies over the last years [1-4]. Advanced fabrication technology has allowed us to study the coupled nanostructures in particular the vertically coupled quantum dots and rings (VCQDs and VCQRs) [3]. Various works have focused on the VCQDs [3]. 1D and 2D approaches applied a lateral geometry with confinement potential, but did not consider effects, such as the geometry, hard wall confinement potential, and non-parabolic band approximation [3]. It should be examined when studying the tunneling ability and the electronic structure by dot-to-dot electronic entanglement and the charge transferability. In exploring the physical properties of these systems, 3D modeling definitely plays a significant role.

With a unified 3D modeling and simulation we for the first time study the inter-distance *d*, structure size and shape, and the magnetic field **B** effects on the electronic structure for VCQDs and VCQRs systematically. It is found that there are quite different energy transition phenomena depending on *d* and the applied **B** between the structures.

2. Theoretical Model and Solution Method

As shown in Figs. 1 and 5, the disk- and conical-shaped (DI- and CO-shaped) InAs/GaAs semiconductor VCQD and VCQR are investigated. Our model considers: (1) the effective 3D one-electronic-band Hamiltonian, (2) the energy- and position-dependent approximation for electron effective mass and Landé factor, (3) the finite hard wall confinement potential, and (4) the Ben Daniel-Duke boundary conditions. For a system in the one-band envelope-function formalism, effective Hamiltonian is [4]

$$\hat{H} = \boldsymbol{\Pi}_{\mathbf{r}} \frac{1}{2m(E,\mathbf{r})} \boldsymbol{\Pi}_{\mathbf{r}} + V(\mathbf{r}) + \frac{1}{2} g(E,\mathbf{r}) \mu_B \mathbf{B}\boldsymbol{\sigma} \qquad (1)$$

where $\boldsymbol{\Pi}_{\mathbf{r}}$ is the electron momentum vector, V(r) is the confinement potential, $m(E,\mathbf{r})$ and $g(E,\mathbf{r})$ are the electron effective mass and Landé factor [4]. The hard-wall confinement potential in the system (S) and environmental crystal matrix (M) is: $V_i(\mathbf{r}) = 0$ for all $\mathbf{r}$ in S and $V_i(\mathbf{r}) = V_{i0}$ for all $\mathbf{r}$ in M. $\boldsymbol{\sigma}$ is the vector of the Pauli matrix. The Ben Daniel-Duke boundary condition for the electron wavefunction $\Psi(\mathbf{r})$ between material interface $\mathbf{r}_s$ is

$$\Psi_1(\mathbf{r}_s) = \Psi_2(\mathbf{r}_s) \text{ and } \left\{ \frac{\hbar^2}{2m(E,\mathbf{r})} \nabla_{\mathbf{r}} \right\}_n \Psi(\mathbf{r}_s) = \text{constant.} \qquad (2)$$

Without any artificial fitting parameters, the derived problem (1)-(2) is solved self-consistently with a generalized nonlinear iterative method [4]. From our experience it solves complicated nanostructures efficiently.

3. Results and Discussion

In our investigation, all nanostructures have the same volume and the radius R (R^{dot} = 100 A^o, R_{in}^{ring} = 100 A^o, and R^{ring} = 200 A^o [1-4]) is fixed for all shapes. Figs. 2 and 6 are the electron transition energy versus *d* for the VCQDs and VCQRs at **B** = 0 T. For a fixed structure volume, radii, and *d*, the electron wavefunction is well confined in the DI-shaped VCQR. This produces a sizable energy (angular momentum l = 0) variation (Fig. 6a) among the structures when *d* is changed. We also find the VCQRs have larger tunneling ability than that of the VCQDs. We note that for CO-shaped VCQDs and VCQRs (Figs. 2b and 6b.), the first excited state ($|l|$ = 1) energy is less dependent on *d*. Figs. 3 and 7 clearly confirm the wavefunction localizations. For a fixed *d*, as shown in Figs. 4 and 8, the electron energy states of the VCQRs strongly depend on the applied **B** and have a transition between configurations with the lowest energy state corresponding to l = 0,-1,-2, … and spin = +1/2. It is found that the DI-shaped VCQR (Fig. 8a) has significantly nonperiodical Aharonov-Bohm oscillation [2,4] which does not obey the well-known 1D periodical rule. This transition energy of VCQRs relates to the persistent current and is useful in optical-magneto devices [1-3]. We observe that the first fracture Φ_c of the VCQRs is greater than the commonly quoted value $\Phi_0/2$ (Φ_0 is the quantum of magnetic flux). However, as shown in Fig. 4 both the VCQDs have the diamagnetic shifts slightly when the applied **B** increases [4].

4. Conclusions

In summary, the topology and magnetic field effects on the electronic structure for nanoscale InAs/GaAs VCQDs and VCQRs has been explored. With the developed 3D simulator, we have found different dependence of *d* and **B** for these nanostructures. The electron wavefunction is well confined in the DI-shaped VCQR, so among structures it has largeste energy variation when *d* is changed. When **B** is applied, the DI-shaped VCQR also shows a strongly nonperiodical transition oscillation.

Acknowledgements

This work is supported in part by the grants: NSC 91-2112-M-317-001 and PSOC 91-EC-17-A-07-S1-0011 in Taiwan.

References

[1] H. Akinaga and H. Ohno, IEEE T. Nanotech., **1** 19 (2002); A. Fuhrer, et al., Nature **413** 822 (2001); D. Bimberg, et al., Thin Solid Films **367** 235 (2000).
[2] R. Blossey, et al., Phys. Rev. E **65** 021603 (2002); A. Lorke, et al., Phys. Rev. L **84** 2223 (2000); A. Emperador, et al., Phys. Rev. B **62** 4573 (2000); A. Bruno-Alfonso, et al., Phys. Rev. B **61** 15887 (2000); A. Fuhrer, et al., Microelec. Eng. **63** 47 (2002).
[3] X. Hu, et al., Phys. Rev. A 61 062301 (2000); P. Yu, et al., Phys. Rev. B 60 16680 (1999); W. Xie, et al., Phys. Lett. A **245** 297 (1998).
[4] Y. Li, et al., Jpn. J. App. Phys. **41** 2698 (2002); Comput. Phys. Commun. **147** 209 (2002); Extended Abstract of SSDM 2002, p. 574.

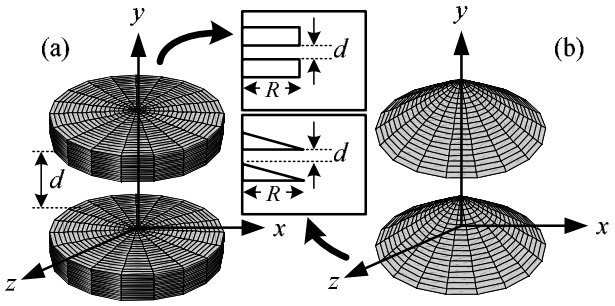

Fig. 1. Three-dimensional and cross section plots for (a) DI- and (b) CO-shaped InAs/GaAs quantum dots.

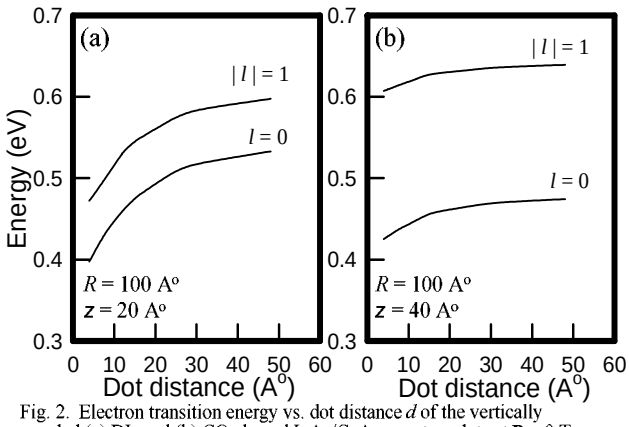

Fig. 2. Electron transition energy vs. dot distance d of the vertically coupled (a) DI- and (b) CO-shaped InAs/GaAs quantum dots at $\mathbf{B} = 0$ T.

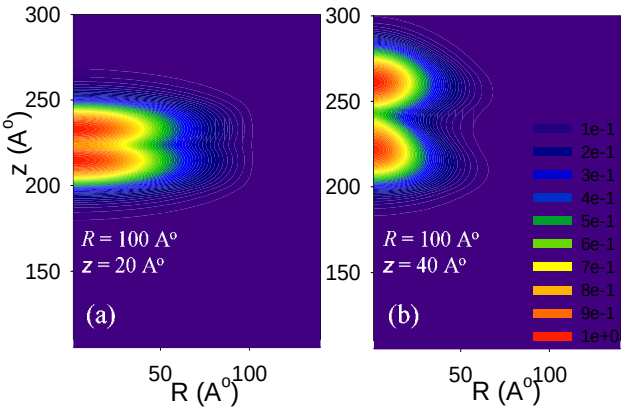

Fig. 3. Electron wavefunction of the vertically coupled DI- (a) and the CO-shaped (b) InAs/GaAs quantum dots for $l = 0$ and $\mathbf{B} = 0$ T.

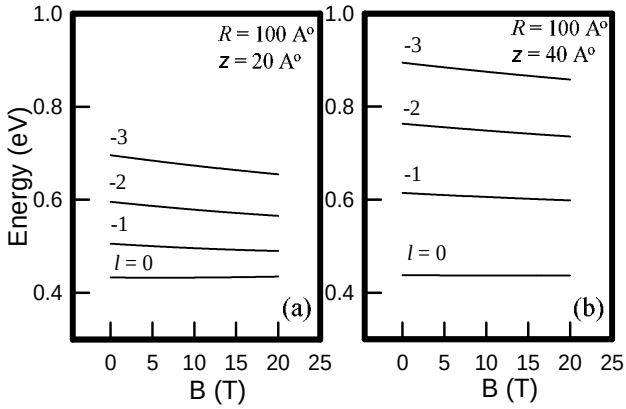

Fig. 4. Electron transition energy vs. magnetic field $\mathbf{B}$ of the vertically coupled (a) DI- and (b) CO-shaped InAs/GaAs quantum dots where d = 8 A°.

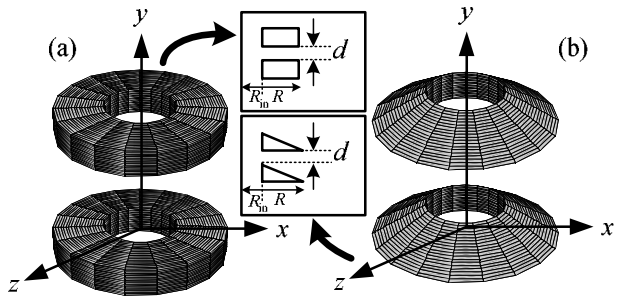

Fig. 5. Three-dimensional and cross section plots for (a) DI- and (b) CO-shaped InAs/GaAs quantum rings.

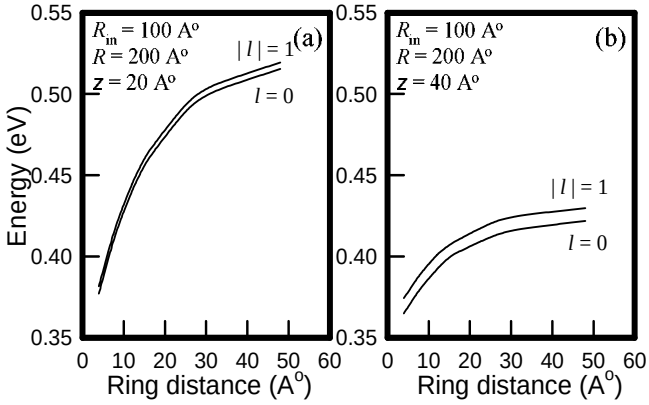

Fig. 6. Electron transition energy vs. ring distance d for the vertically coupled (a) DI- and (b) CO-shaped InAs/GaAs quantum rings at $\mathbf{B} = 0$ T.

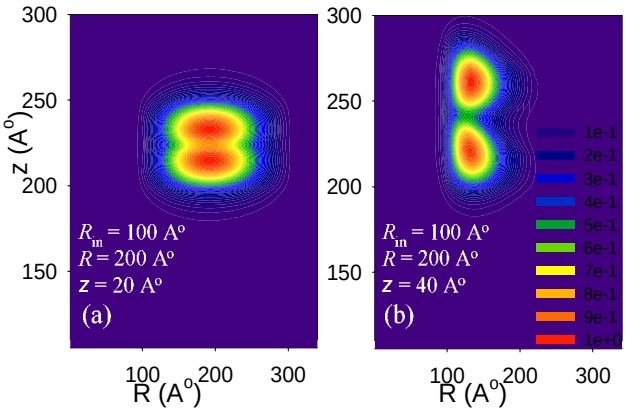

Fig. 7. Electron wavefunction of the vertically coupled DI- (a) and the CO-shaped (b) InAs/GaAs quantum rings for $l = 0$ and $\mathbf{B} = 0$ T.

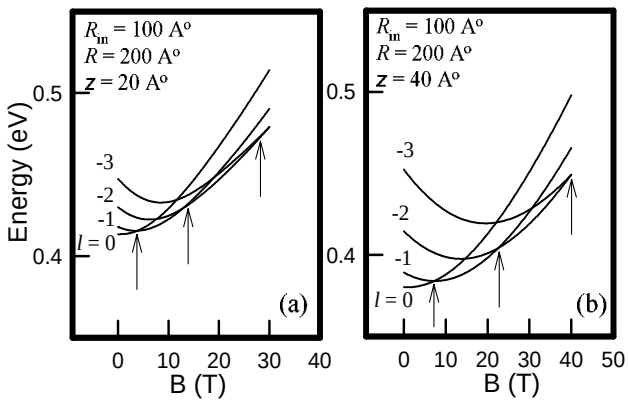

Fig. 8. Electron transition energy vs. magnetic field $\mathbf{B}$ of the vertically coupled (a) DI- and (b) CO-shaped InAs/GaAs quantum rings where d = 8 A°.